Responses to Anonymous Referee #1

We thank the Anonymous Referee #1 for their time and effort to review our manuscript, which helped to further increase the quality of the paper. All comments have been addressed carefully.

Below, reviewer comments are marked in red.
Responses to the comments are marked in blue.
Changes that have been made in the manuscript are marked in *italic*.

Major Comments

1. Given the potential for extensive use in long-term ecological applications due to its 35-year timespan (1987-2021), ensuring consistency throughout the VODCA CXKu & L data is paramount. To this end, I strongly recommend including yearly time series of VODCA CXKu / L at global, continental, or landcover scales.

We thank the reviewer for this valuable comment and agree that the consistency of VODCA v2 products in space and time is critical, given the potential and likely user uptake for long-term ecological applications. Therefore, we added a dedicated section in the Chapter Results, "Spatio-temporal consistency".

To ensure that the merging of multiple sensors and frequencies has not affected the consistency of VOD through time and space, we have computed several additional analyses:

- Global and hemispherical plots showing the yearly average, yearly anomalies and yearly percentage of valid observations (Figs. 1, 2). These have been calculated from the yearly averages weighted by the cosine of the latitude.
- Time-latitude plots showing the mean monthly VOD (Fig. 3).
- Time-latitude plots showing the monthly anomalies (Fig. 4) with respect to the reference period 1990 - 2020. The anomalies were calculated by the following steps: collecting all observations for a given latitude, determining the monthly mean, subtracting the multi-year monthly average, and eliminating any potential linear trends using ordinary least-squares regression. Therefore, anomalies should represent either natural variability or artefacts due to changes in the sensor constellation.
- Time-latitude plots showing the first-order autocorrelation (AC(1)) of VOD observations in each year (Fig. 5). These were calculated by collecting all observations for a given latitude, filling in missing observations using linear interpolation because AC(1) coefficients strongly depend on the temporal resolution (Moesinger et al., 2020), and calculating the yearly AC(1). We rely on the assertion that there should be a high degree of temporal AC(1) between subsequent observations since VOD is related to gradual changes in plant water content and biomass (Momen et al. (2017), Konings et al. (2016), Moesinger et al. (2020)). Therefore, in Fig. 5, a decrease in AC(1) coincident with the timing of introducing a new sensor would indicate that the merging has led to larger random errors in the product. Similarly, an increase would suggest that the merging has led to lower random error levels.

The global and hemisphere mean VOD plots show no breaks when new sensors are introduced in either VODCA CXKu (Fig. 1) or VODCA L (Fig. 2). Therefore, we attribute the changes in VOD to natural variability. Concerning VODCA CXKu, anomalies have been observed to coincide with El Niño-Southern Oscillation (ENSO) variations (Dorigo et al. (2021), Dorigo et al. (2022), Zotta et al. (2023)) especially in the Southern Hemisphere, where there is a clear connection between ENSO and vegetation activity (Martens et al. (2017)). Regarding the bulk signal, we can observe a clear positive trend in VODCA CXKu, consistent with reports on global greening based on different and independent satellite sources (e.g., Piao et al. (2020), Chen et al. (2024), Zhang et al. (2017)).

The seasonal dynamics of VODCA CXKu over time and space (Fig. 3 upper) show consistent patterns, with higher VOD in the summer months due to the increase in temperature (in the northern-southern region) or in precipitation (in the subtropics). In VODCA L (Fig. 3 lower), the seasonal patterns are less prevalent, which is to be expected because it also contains information on the woody components of the vegetation layer, which is more constant throughout the year. The seasonality and magnitude of VOD are consistent over time and space in both datasets. Most anomalies in VODCA CXKu and VODCA L (4) appear limited in time, and their start and end do not coincide with sensor changes, thus indicating natural variability. Moreover, the anomaly patterns of VODCA CXKu are very similar to those of MODIS fAPAR (Fig. 6). The yearly AC(1) appears consistent through time in VODCA CXKu (Fig. 5 upper), with some latitudes experiencing a slight increase at approximately 30 - 60 N and 0 - -30 N coincident with the introduction of AMSR-E (Jun. 2002) and TMI (Dec. 1997). At the same time, no consistent decreases in AC(1) can be observed, suggesting that no sensor has led to an increase in random error compared to the previous state of the product. In VODCA L (Fig. 5), we see an increase in AC(1) in almost all latitudes coincident with the introduction of SMAP (Mar. 2015). These results suggest that fusing observations in the overlapping period has led to a more robust product in terms of random error than using only SMOS observations. As a result of this analysis, we reiterate that we expected to see to some degree a change in AC(1) with the merging of sensors, as VODCA CXKu and VODCA L are harmonized (through the removal of bias between sensors and fusion of overlapping observations) but not homogenized (forcing same data characteristics throughout the entire period covered by the merged product). Therefore, as already mentioned in the manuscript, it is crucial to consider the influence of heterogeneous sensor constellation through time for research that delves into higher-order statistics such as variance and autocorrelation temporally (Smith et al., 2022).

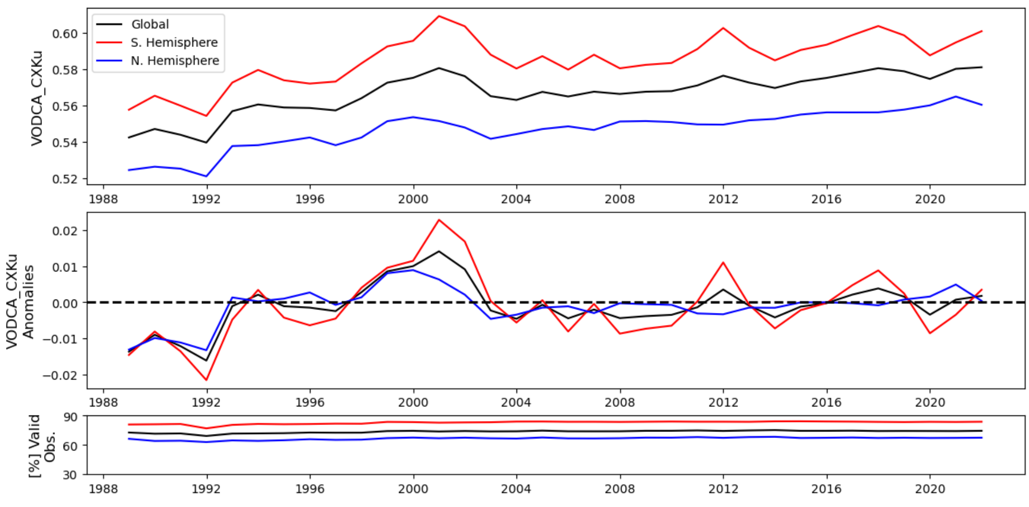

Figure 1: Global and hemisphere time-series of VODCA CXKu.

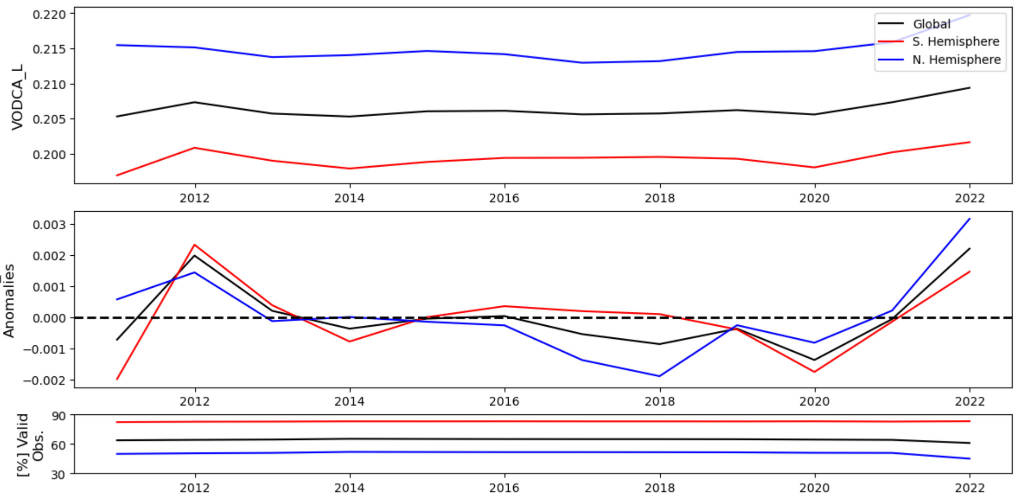

Figure 2: Global and hemisphere time-series of VODCA L.

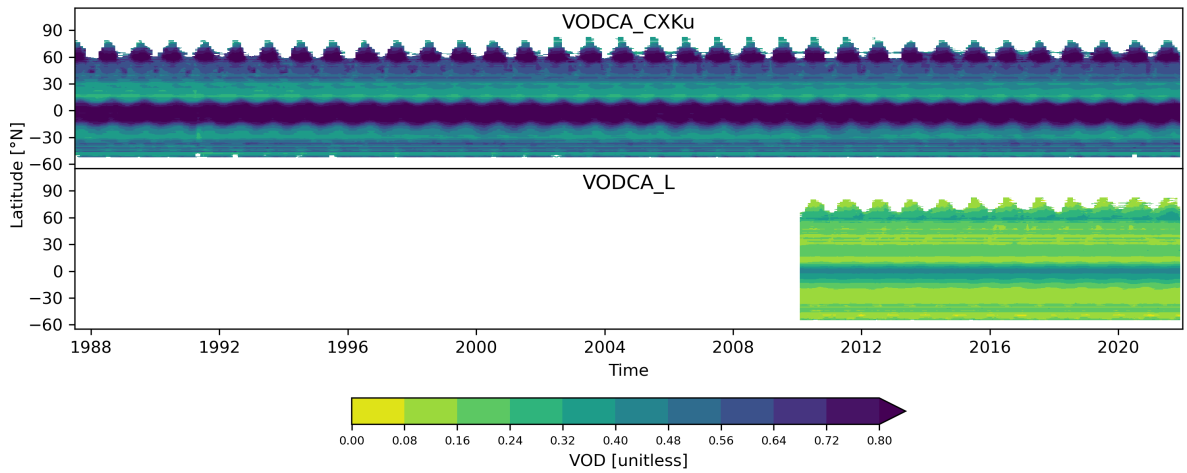

Figure 3: Hovmöller diagrams showing the monthly mean VOD per latitude for VODCA CXKu and VODCA L.

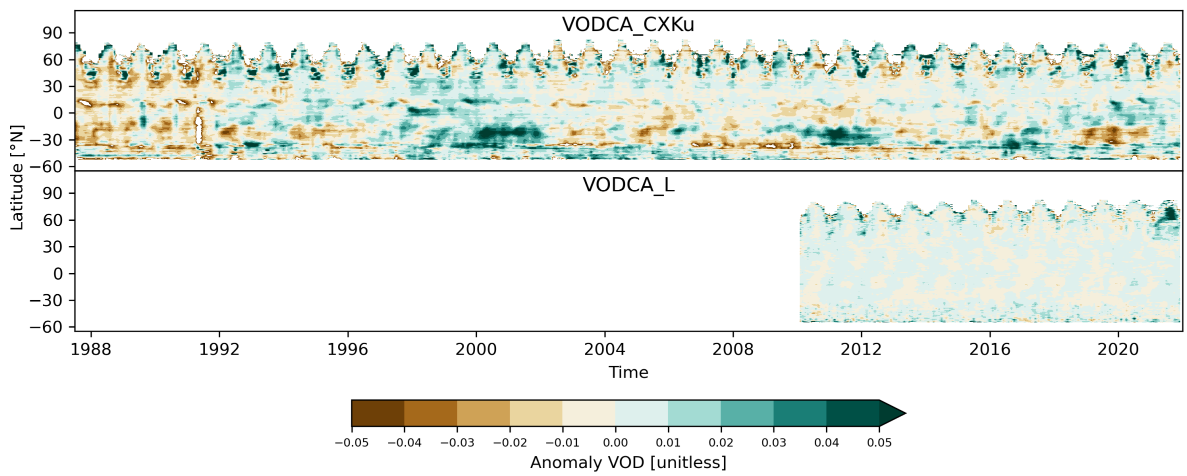

Figure 4: Hovmöller diagrams showing anomalies of the monthly means per latitude for VODCA CXKu and VODCA L.

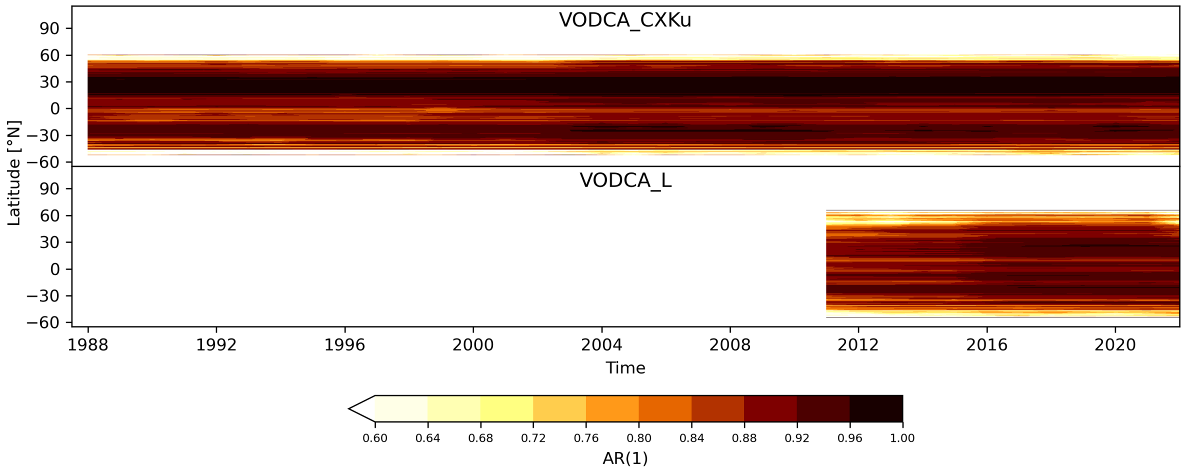

Figure 5: Hovmöller diagrams showing the yearly AC(1) per latitude for VODCA CXKu and VODCA L.

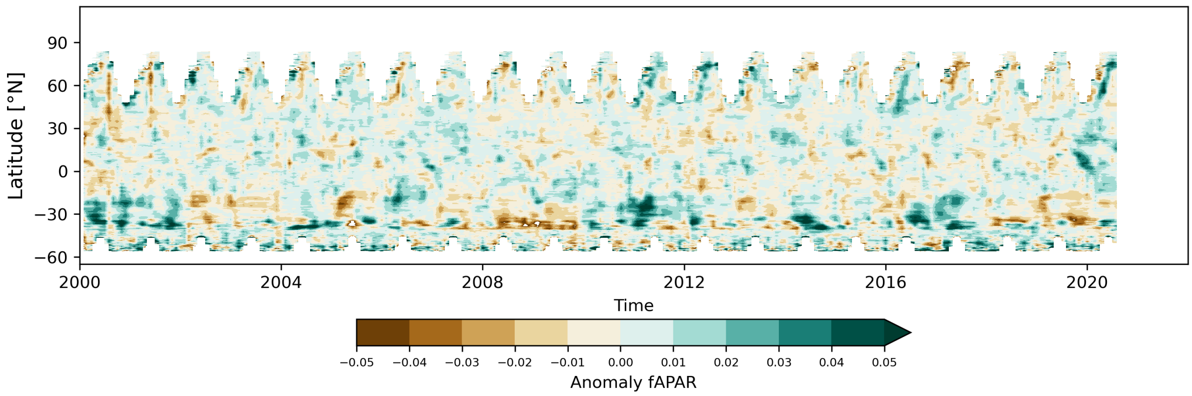

Figure 6: Hovmöller diagrams showing anomalies of the monthly means per latitude for MODIS fAPAR.

We introduced a new section in the Chapter Results (Chapter 4.2), "Spatio-temporal consistency", that presents the abovementioned results. We include Figures 3, 4 and 5 in Chapter 4.2. We include the global and hemisphere time series (Fig. 1, VODCA CXKu) and (Fig. 2, VODCA L) in the Annex, as well as the time-latitude plot showing fAPAR (Fig. 6).

Minor Comments

1. Line 15: does the canopy include trunks?

We found conflicting information based on the domain (biology vs. forest ecology) concerning the definition of the canopy. To avoid confusion, we defined it in line 15 of the original manuscript as including branches and trunks.

2. Line 125 "Ku-band (19.4 GHz)" and "Ku-band (18.7 GHz)", microwave at 19.4 GHz and 18.7 GHz belongs to K-band (18-27 Ghz), why "Ku-band" was used in this ms?

Thank you very much for your comment. Indeed, both frequencies used belong to the K-band.

We are using the 18.7 GHz band, which is at the edge of the K band. Some sensors, such as AMSR2, also provide the 23.6 GHz band from the middle of the K band. Therefore, we call the 18.7 GHz band Ku-band to differentiate between these K-band frequencies. This notation has been used within the framework of the European Space Agency Climate Change Initiative (CCI) (`https://climate.esa.int/en/projects/soil-moisture/`) and the Copernicus Climate Change Service (C3S) (`https://climate.copernicus.eu/`), and we adopted it since the single-sensor VOD data from VODCA is produced in these projects. The notation is used throughout the CCI Soil Moisture ATBD in Dorigo et al. (2017). Moreover, many independent studies which use data in the 18.7 GHz and 19.4 GHz frequencies use the terminology Ku-band (e.g., Fan et al. (2018), Santi et al. (2017)).

References

Chen, X., Chen, T., He, B., Liu, S., Zhou, S., and Shi, T.: The global greening continues despite increased drought stress since 2000, Global Ecology and Conservation, 49, e02 791, 2024.

Dorigo, W., Wagner, W., Albergel, C., Albrecht, F., Balsamo, G., Brocca, L., Chung, D., Ertl, M., Forkel, M., Gruber, A., et al.: ESA CCI Soil Moisture for improved Earth system understanding: State-of-the art and future directions, Remote Sensing of Environment, 203, 185–215, 2017.

Fan, L., Wigneron, J.-P., Xiao, Q., Al-Yaari, A., Wen, J., Martin-StPaul, N., Dupuy, J.-L., Pimont, F., Al Bitar, A., Fernandez-Moran, R., et al.: Evaluation of microwave remote sensing for monitoring live fuel moisture content in the Mediterranean region, Remote Sensing of Environment, 205, 210–223, 2018.

Konings, A. G., Piles, M., Rötzer, K., McColl, K. A., Chan, S. K., and Entekhabi, D.: Vegetation optical depth and scattering albedo retrieval using time series of dual-polarized L-band radiometer observations, Remote sensing of environment, 172, 178–189, 2016.

Martens, B., Miralles, D. G., Lievens, H., Van Der Schalie, R., De Jeu, R. A., Fernández-Prieto, D., Beck, H. E., Dorigo, W. A., and Verhoest, N. E.: GLEAM v3: Satellite-based land evaporation and root-zone soil moisture, Geoscientific Model Development, 10, 1903–1925, 2017.

Moesinger, L., Dorigo, W., de Jeu, R., van der Schalie, R., Scanlon, T., Teubner, I., and Forkel, M.: The global long-term microwave vegetation optical depth climate archive (VODCA), Earth System Science Data, 12, 177–196, 2020.

Momen, M., Wood, J. D., Novick, K. A., Pangle, R., Pockman, W. T., McDowell, N. G., and Konings, A. G.: Interacting effects of leaf water potential and biomass on vegetation optical depth, Journal of Geophysical Research: Biogeosciences, 122, 3031–3046, 2017.

Piao, S., Wang, X., Park, T., Chen, C., Lian, X., He, Y., Bjerke, J. W., Chen, A., Ciais, P., Tømmervik, H., et al.: Characteristics, drivers and feedbacks of global greening, Nature Reviews Earth & Environment, 1, 14–27, 2020.

Santi, E., Paloscia, S., Pampaloni, P., Pettinato, S., Nomaki, T., Seki, M., Sekiya, K., and Maeda, T.: Vegetation water content retrieval by means of multifrequency microwave acquisitions from AMSR2, IEEE Journal of Selected Topics in Applied Earth Observations and Remote Sensing, 10, 3861–3873, 2017.

Smith, T., Traxl, D., and Boers, N.: Empirical evidence for recent global shifts in vegetation resilience, Nature Climate Change, 12, 477–484, 2022.

Zhang, Y., Song, C., Band, L. E., Sun, G., and Li, J.: Reanalysis of global terrestrial vegetation trends from MODIS products: Browning or greening?, Remote Sensing of Environment, 191, 145–155, 2017.